Chemical Science

ROYAL SOCIETY OF CHEMISTRY

EDGE ARTICLE

View Article Online
View Journal | View Issue





Cite this: *Chem. Sci.*, 2020, **11**, 6325

All publication charges for this article have been paid for by the Royal Society of Chemistry

Received 13th May 2020
Accepted 4th June 2020

DOI: 10.1039/d0sc02745f

rsc.li/chemical-science

# Reversible photo-control over transmembrane anion transport using visible-light responsive supramolecular carriers†

Aidan Kerckhoffs and Matthew J. Langton *

Ion transport across lipid bilayer membranes in biology is controlled by membrane proteins, which in turn are regulated in response to chemical-, physical- and photo-stimuli. The design of synthetic supramolecular ion transporters able to be precisely controlled by external signals, in particular biocompatible wavelengths of visible light, is key for achieving spatio-temporal control over function. Here we report two-colour responsive molecular photo-switches that act as supramolecular transmembrane anion carriers. Reversible switching of the photo-switch within the lipid bilayer membrane is achieved using biocompatible visible wavelengths of light, such that temporal control over transmembrane anion transport is achieved through alternating irradiation with red and blue light.

## Introduction

Ion transport across lipid bilayer membranes in biology is regulated by membrane proteins, which are themselves regulated by external stimuli such as small molecules, membrane potential and light. Protein ion channels and their modified analogues find applications in diverse fields ranging from optogenetics,[1] photopharmacology,[2] and synthetic biology.[3] Supramolecular anionophores that act as mobile ion carriers have also attracted significant interest; driven by potential uses as therapeutics for cancer treatment and diseases arising from mis-regulated ion channels including cystic fibrosis, or as tools for studying ion transport processes.[4] Significant effort has been devoted to designing mobile carrier systems with high anion transport activity in vesicles and, more recently, in cells.[5]

Whilst the activity of natural ion channels and transporters can be precisely controlled by external stimuli, stimuli-responsive supramolecular ion channels[6] and mobile ion carriers[7] are rare, and achieving high levels of control (to switch between inactive "OFF" states and ion transporting "ON" states) is particularly challenging. Photo-regulated transporters are particularly attractive targets, because of the possibility of achieving both spatial and temporal control over ion transport in a readily adaptable synthetic system. Since the pioneering work of Shinkai and co-workers on photo-controlled cation transport in liquid membranes,[8] the large amplitude conformational change afforded by *E*–*Z* photo-isomerisation has been a key component of many light-activated molecular machines, receptors and catalysts.[9] However, light-activated mobile ion carriers that function in lipid bilayers are extremely rare, and precise, reversible control over activity is particularly challenging to achieve. Furthermore, the photo-responsive ion carriers reported to date employ almost exclusively UV light-triggered transport mechanisms.[7e–g] UV-light is generally unsuitable for biological applications due to poor tissue penetration and collateral cell damage.[2a] Because of this limitation, long wavelength visible light photo-switches are attracting significant interest as tools for chemical biology applications.[10] Here we report a supramolecular photo-switchable carrier able to regulate transmembrane anion transport using visible light. The system is reversibly controlled by alternate irradiation with red and blue light, with a high level of discrimination between the OFF and ON states.

## Results and discussion

### Approach

Synthetic mobile ion carriers facilitate ion transport down a concentration gradient by lowering the kinetic barrier to transmembrane transport. This is achieved through binding of the ion within a hydrophobic receptor, which diffuses across the bilayer to release the ion on the opposite side. For the development of reversible photo-controlled anion carriers, we identified two key requirements: (i) excellent discrimination between the inactive "OFF" state (with negligible background transport) and photo-activated "ON" state and (ii) photo-switching with visible light for improved biocompatibility. Efficient anion transporters require sufficient lipophilicity to ensure optimum partitioning into the membrane, excellent anion binding affinity,[11] and also benefit from encapsulation of the hydrophilic anion within a hydrophobic receptor.[12]

*Chemistry Research Laboratory, University of Oxford, Mansfield Road, Oxford, OX1 3TA, UK. E-mail: matthew.langton@chem.ox.ac.uk*

† Electronic supplementary information (ESI) available. See DOI: 10.1039/d0sc02745f

Conversely, carriers with weak anion binding affinity, poor encapsulation and extended conformations typically exhibit low activity; the latter attributed to reduced mobility and high reorganization penalties within the membrane.[13]

We identified red-shifted azobenzenes bearing anion binding groups of the general structure **1** (Fig. 1) as a possible scaffold that fulfils these requirements, where *E*–*Z* photo-isomerization of azobenzenes is exploited to enhance anion recognition by cooperative binding between two appended receptors. A greater degree of anion encapsulation and increased mobility of the less extended *Z* isomer relative to the *E* isomer enhances the anion transport capability further.

## Design and synthesis

The *E*–*Z* photo-isomerisation of azobenzenes is achieved using UV light and reversed with visible light or by thermal relaxation; the rate of which depends on the substituents but can often be fast ($t_{1/2}$ milliseconds to minutes).[14] To address the key challenge of achieving reversible, visible light mediated control over ion transport, we designed molecular photo-switches incorporating *ortho*-chloro-substituted azobenzene derivatives. Recent work by a number of groups including those of Hecht and Woolley has demonstrated that heteroatom *ortho*-substitution of azobenzenes leads to significant red shifting of the n–π* band of the *E* isomer, separating it from the *Z* n–π* transition.[15] This allows for bi-directional photo-switching with orthogonal wavelengths of visible light, and significantly enhanced *Z* isomer lifetimes. Remarkably, *ortho*-chloro-derivatives have been shown to allow photo-switching with red light, which is highly beneficial for biological applications.[15d]

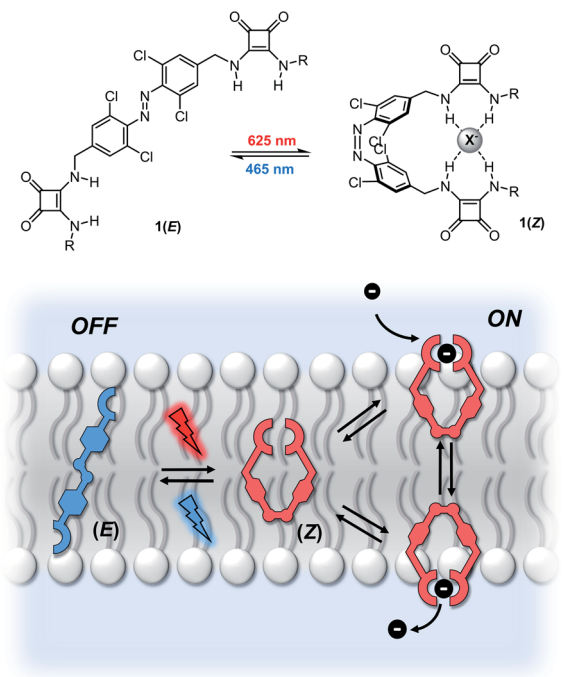


Fig. 1 Schematic representation of two-colour photo-switching of a supramolecular ion carrier **1**.

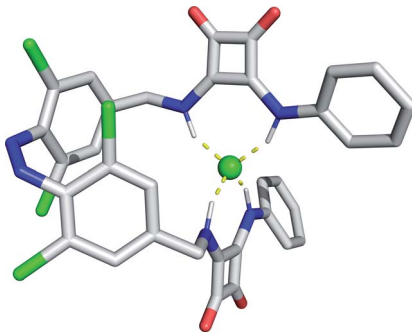

Fig. 2 Calculated structure of the chloride complex $\mathbf{1a}^{Z}\cdot$Cl (MM+ force field, HyperChem).

Direct conjugation of anion binding motifs to the azobenzene core is known to significantly decrease the lifetime of the *Z* isomer (such as in azobenzene-urea derivatives).[16] Molecular mechanics calculations indicated that incorporation of methylene spacers between the photo-switch and the anion binding squaramides allows for cooperative chloride anion binding between both squaramide motifs in the *Z* isomer (Fig. 2). Squaramides are potent halide ion binders, and highly effective anion transporters.[17]

Red-shifted azobenzene derivatives **1a–i** were prepared as shown in Scheme 1. Reduction and immediate protection of 4-cyano-2,6-dichloroaniline **2** afforded **3**, which was subjected to oxidative coupling conditions[18] to afford red-shifted azobenzene **4** in good yields. Quantitative Boc-deprotection gave rise to **5**, which was subsequently reacted with mono-squaramide derivatives (**6a–i**, prepared from dimethyl squarate and the corresponding amine derivative), to afford the

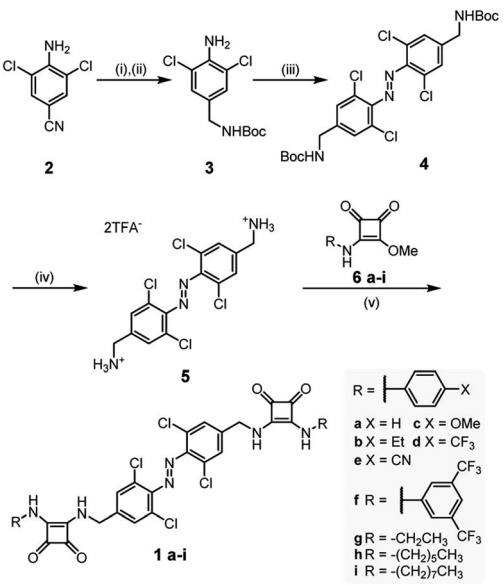


Scheme 1 Synthesis of squaramide-functionalized azobenzene anion carriers. Conditions: (i) $LiAlH_4$, THF, 3 h, rt; (ii) $Boc_2O$, THF, 3 h, rt, 59% over two steps; (iii) NCS, DBU, $CH_2Cl_2$, 10 min, −78 °C, 43%; (iv) TFA, $CH_2Cl_2$, 4 h, quant.; (v) **6a–i**; DIPEA, MeOH, 16 h, 55 °C, 49–83%.

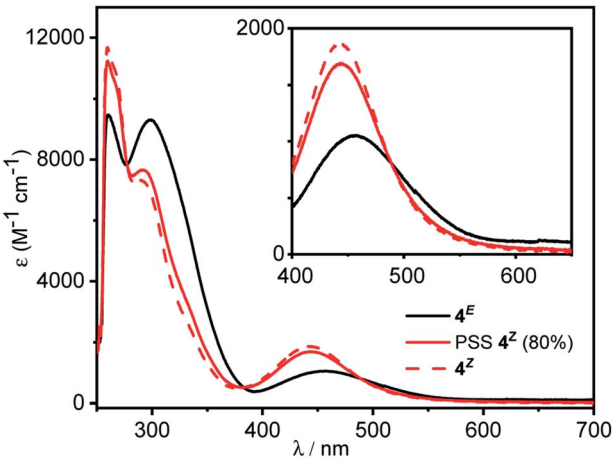


Fig. 3 Absorption spectra of **4** as the *E* and *Z* isomer, as well as the PSS mixture in DMSO at 25 °C. Inset: n → π* bands and composition of the PSS mixtures upon irradiation with red light (625 nm, determined by NMR integration). Pure Z-isomer spectrum was calculated from the spectra of pure $\mathbf{4}^{E}$ and the PSS mixture of known composition.

anion carriers **1a–i**. For full experimental procedures and characterization see the ESI.†

We first examined the photo-switching properties of the parent azobenzene **4**. Irradiation of $\mathbf{4}^{E}$ with red light from an LED (625 nm, ~0.9 W) allowed for high conversion to the *Z* isomer in the photo-stationary state (PSS) (80% $\mathbf{4}^{Z}$ as determined by NMR integration). The UV-vis spectra of $\mathbf{4}^{E}$ and $\mathbf{4}^{Z}$ are shown in Fig. 3. As with similar *ortho*-chloro-substituted azobenzenes,[15d] significant red-shifting of the n–π* transition is observed, and separation of the *E* n–π* from the *Z* n–π* transitions allows for efficient switching (Fig. 2). Irradiation with blue light (LED, 455 nm, ~1.1 W) was effective at triggering the reverse *Z* → *E* photo-isomerisation (86% *Z* → *E*). The *Z* isomer exhibited excellent thermal stability, with a half-life for the thermally promoted *Z* → *E* isomerization of ~7 days at 298 K (Fig. S78†).

## NMR anion binding titrations

With the library of squaramide-functionalized bistable switches in hand, we examined their chloride binding capability by conducting $^{1}$H NMR titration experiments in $d_6$-DMSO by addition of aliquots of tetrabutylammonium chloride, and monitoring the binding induced chemical shift perturbations. Data were fitted to the appropriate binding isotherms using the Dynafit software package,[19] and the association constants are shown in Table 1. $K_1^E$ is the 1 : 1 binding constant for chloride recognition by one squaramide motif of the bi-functional *E*-isomer, weighted by the appropriate statistical factor, and $K_1^Z$ is the corresponding 1 : 1 binding constant for chloride recognition by the *Z* isomer. The latter were determined by repeating the titration with the PSS mixture formed by irradiating the sample in the NMR tube with 625 nm light (77% *Z* for **1a–i**), and accounting for the binding competition to the minor population of *E* isomer in the analysis (see ESI† for data and binding models). The affinity of $\mathbf{1}^{E}$ for chloride was relatively weak in this competitive polar solvent, and binding of a second equivalent of anion was too weak to be determined, presumably due to unfavourable anion–anion repulsion. The affinity of $\mathbf{1}^{Z}$ derivatives for chloride were higher than the analogous $\mathbf{1}^{E}$ isomers, with a ratio of $K_1^Z/K_1^E \sim 3$, indicating cooperative anion binding by both squaramide motifs in the *Z* isomer, consistent with the calculated structure. Varying the electron donating or withdrawing nature of the squaramide translated into changes in the binding affinity for chloride in both *E* and *Z* isomers, and for the aryl substituents this showed good correlation with Hammett constant[20] (Fig. 4).

## Anion transport studies

The anion transport activities of the derivatives of **1** were determined in 1-palmitoyl-2-oleoyl-*sn-glycero*-3-phosphocholine large unilamellar vesicles (POPC LUVs, lipid concentration 31 μM), loaded with 8-hydroxypyrene-1,3,6-trisulfonate (HPTS) buffered to pH 7.0 in NaCl solution. A pH gradient was applied across the membrane by addition of a base pulse, followed by

Table 1 Characteristics of photo-switchable anion carriers **1**

| | | Carriers | | | | | | | | |
|---|---|---|---|---|---|---|---|---|---|---|
| Entry | Characteristic | **1a** | **1b** | **1c** | **1d** | **1e** | **1f** | **1g** | **1h** | **1I** |
| 1 | $K_1^E$ $(M^{-1})^a$ | 90 ± 2 | 72 ± 3 | 77 ± 3 | 126 ± 1 | 137 ± 10 | 139 ± 10 | 47 ± 1 | 65 ± 5 | –[e] |
| 2 | $K_1^Z$ $(M^{-1})^a$ | 267 ± 3 | 201 ± 3 | 231 ± 12 | 346 ± 2 | 358 ± 12 | 402 ± 6 | 142 ± 7 | 204 ± 21 | –[e] |
| 3 | $EC_{50}^E$ $(nM)^b$ | 181 ± 16 | 591 ± 341 | 1020 ± 477 | 146 ± 40 | 232 ± 143 | 246 ± 121 | >5000[f] | 204 ± 42 | >20 000[f] |
| 4 | $EC_{50}^{Z,PSS}$ $(nM)^{b,c}$ | 22 ± 2 | 101 ± 18 | 218 ± 54 | 42 ± 12 | 64 ± 13 | 90 ± 55 | 432 ± 41 | 28 ± 2 | >20 000[f] |
| 5 | $n^{E\,d}$ | 2.6 ± 0.5 | 0.6 ± 0.1 | 0.6 ± 0.1 | 1.0 ± 0.2 | 0.6 ± 0.1 | 0.6 ± 0.1 | —[e] | 0.8 ± 0.1 | –[e] |
| 6 | $n^{Z\,d}$ | 1.1 ± 0.1 | 1.0 ± 0.2 | 0.6 ± 0.1 | 0.8 ± 0.1 | 0.7 ± 0.1 | 0.7 ± 0.1 | 1.4 ± 0.1 | 1.2 ± 0.1 | –[e] |
| 7 | $K_1^Z/K_1^E$ | 3.1 | 2.8 | 3.0 | 2.7 | 2.6 | 2.9 | 3.0 | 3.1 | –[e] |
| 8 | $EC_{50}^{Z,PSS}/EC_{50}^E$ | 8.2 | 5.9 | 4.7 | 3.5 | 3.6 | 2.7 | >10[f] | 7.3 | –[e] |

[a] 1 : 1 association constant for chloride binding in $d_6$-DMSO. $K_1^E$ is statistically corrected to account for affinity to one squaramide, where $K_1^E = K_{obs}/2$. Errors at the 95% confidence limit. [b] Effective concentration to reach 50% of maximal activity in the HPTS assay, in LUVs of POPC (mean diameter 200 nm, lipid concentration 31 μM) loaded with 1 mM HPTS, NaCl (100 mM) and buffered at pH 7.0 with 10 mM HEPES. For compounds of low activity, estimated lower bounds for the $EC_{50}$ value are given. [c] For the *Z* isomer, $EC_{50}^{Z,PSS}$ indicates apparent value achieved by addition of the 77 : 23 *Z*/*E* PSS mixture. [d] Hill coefficient. [e] Not determined. [f] Poor solubility in DMSO prevented full Hill analysis.

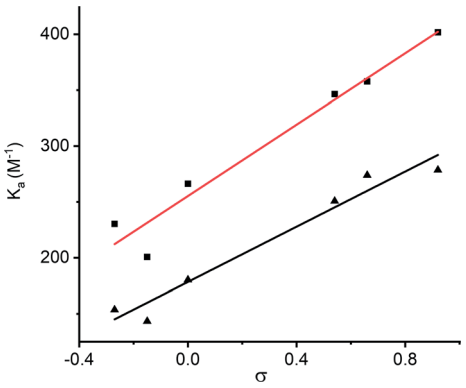


Fig. 4 Plot of *K vs.* Hammett parameter $\sigma$ for aryl derivatives of $\mathbf{1}^E$ and $\mathbf{1}^Z$. Values taken from ref. 20.

addition of the carrier as a DMSO solution (<0.5% v/v). The ability of the anionophore to dissipate the pH gradient by transmembrane ion transport was determined by recording the change in the HPTS emission, $I_{rel}$ ($\lambda_{em}$ = 510 nm), with time following excitation at $\lambda_{ex}$ = 405/465 nm (Fig. 5A). Detergent (Triton X-100) was added at the end of each experiment to lyse the vesicles for calibration. For the *Z* isomers, the experiment was run using the 77 : 23 Z/*E* PSS mixture formed by irradiating the sample with 625 nm light.

The concentration dependence of the activity of the *E* and *Z* isomers of each anion carrier was determined by adding increasing concentrations of the transporter in DMSO. The fractional activities (relative intensity just prior to lysis) were plotted as a function of concentration (Fig. 5B) and the dose–response curves fitted to the Hill equation. This is used to describe the dependence of the anion transport activity (reported by $I_{rel}$) on the *n*-th power of the carrier concentration, and facilitates comparison of the relative activities of carriers through an effective concentration value ($EC_{50}$) required to reach 50% activity.

### Quantifying anion transport activity

The $EC_{50}$ and *n* values for the analogues of $\mathbf{1}^E$, and for the $\mathbf{1}^Z$ enriched PSS (*Z* : *E* 77 : 23) are given in Table 1, entries 3–6; and the corresponding $EC_{50}^{Z,PSS}/EC_{50}^{E}$ ratios (entry 8). A significant enhancement of activity, up to a maximum of 8-fold for compound **1a**, was observed for the *Z* isomers.[21] In general, squaramides with electron withdrawing aryl substituents resulted in efficient transport. The optimal chain length of alkyl derivatives was six carbons, with both ethyl and octyl chains proving detrimental to transport efficiency. The difference in activity between both photo-isomers could be estimated by the ratio $EC_{50}^{Z,PSS}/EC_{50}^{E}$, which was found to be generally higher for the less active compounds, presumably arising from a decreased ability of the *E* isomer to bind and transport anions. In contrast, the ratio of 1 : 1 binding constants, $K_1^Z/K_1^E$, remains consistent at ~3 across the whole family of compounds. We hypothesise that the larger increase in transporter efficiency for the $\mathbf{1}^Z$ derivatives, compared to that predicted by the ratio of binding constants alone, arises in part from reduced mobility of the linear *E* isomer–anion complex in the membrane, and diminished ability to fully encapsulate the anion compared to the *Z* isomer. It has been previously shown that the relationship between anion binding affinity and $EC_{50}$ is complex, often without direct correlation, because transport efficiency is also strongly dependent on other factors including molecular size and hydrophobicity.[11b] The important role of encapsulation in increasing transport affinity has also previously been demonstrated.[12]

Hill coefficients of ~1 for $\mathbf{1}^Z$ analogues suggests ion complexation with a likely 1 : 1 stoichiometry ($\mathbf{1}^Z \cdot Cl^-$) in the transport complex, consistent with results from titration experiments and calculation. Enhanced binding interactions in membranes, arising from two-dimensional confinement and the hydrophobic, low polarity environment,[22] may also allow for competing formation of the *E* isomer 2 : 1 transporter–anion complex ($\mathbf{1}_2^E \cdot Cl^-$), as well as hydrogen bonding aggregates of $\mathbf{1}^E$ in the membrane. Hill coefficients ranging between ~0.6–2.6

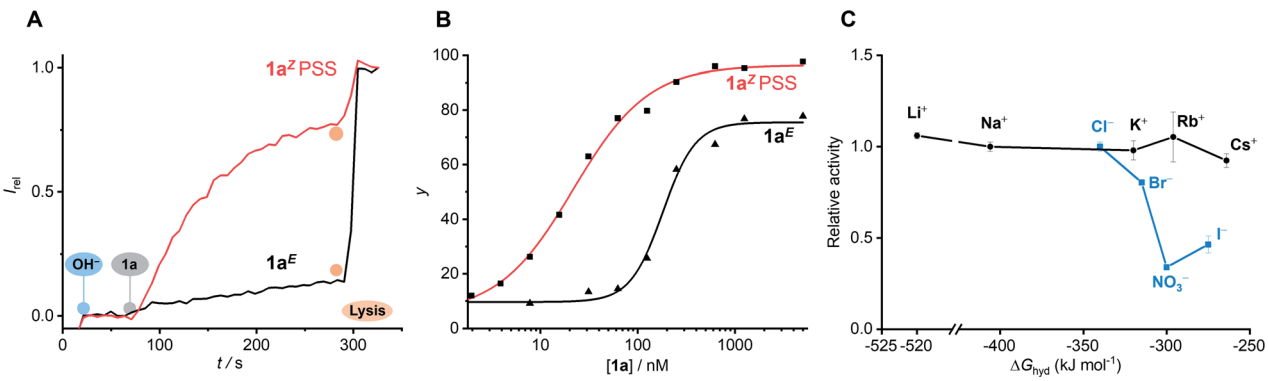


Fig. 5 (A) Change in ratiometric emission ($\lambda_{em}$ = 510 nm; $\lambda_{ex1}$ = 405 nm, $\lambda_{ex2}$ = 460 nm) upon addition of 62.5 nM $\mathbf{1a}^E$ (black) and $\mathbf{1a}^Z$ (red) in DMSO to POPC LUVs (31 μM) containing 1 mM HPTS, 100 mM internal and external NaCl, buffered with 10 mM HEPES at pH 7.0. A pH gradient is generated by addition of a NaOH base pulse (5 mM), followed by **1a** in DMSO. Lysis by Triton X-100 calibrates the assay. (B) Dependence on $I_{rel}$ immediately prior to lysis on concentration of $\mathbf{1a}^E$ (▲) and $\mathbf{1a}^Z$ (■), and fit to the Hill equation (solid line). (C) Dependence of the activity of $\mathbf{1a}^Z$ (62.5 nM) on extra-vesicular ions (100 mM MCl or NaX; inside 100 mM NaCl). Error bars represent standard deviations. Original data for all other compounds is available in the ESI.†

are indicative of a range of competing equilibria in the membrane for the $\mathbf{1}^{E}$ isomer derivatives, with $n < 1$ arising from competing formation of inactive complexes and/or precipitation at high concentrations.[23] Compound **1a** provides a balance between good $EC_{50}^{Z}/EC_{50}^{E}$ discrimination and overall high activity as the *Z* isomer ($EC_{50}$ of 22 nM, 0.07 mol% relative to the lipids), and was used for analysis in subsequent experiments.

### Ion selectivity and mechanistic studies

The activity of transporter $\mathbf{1a}^{Z}$ was unaffected by iso-osmolar replacement[24] of the external $Na^+$ cation with $Li^+$, $K^+$, $Rb^+$ or $Cs^+$, but was sensitive to replacement of the external $Cl^-$ anion with $Br^-$, $I^-$ or $NO_3^-$ (Fig. 5C). No observable transport was detected when chloride was replaced with gluconate, a large hydrophilic anion,[12] suggesting that $\mathbf{1a}^{Z}$ is unable to overcome the large dehydration penalty required for $OH^-$/gluconate$^-$ antiport (Fig. S138†). Diminished activity with anionic lipids (egg yolk phosphatidylglycerol) was also consistent with the requirement for formation of an anionic complex $\mathbf{1}^{Z}\cdot Cl^-$, due to charge repulsion with the membrane (Fig. S139†). Together, these results demonstrate that the dissipation of the pH gradient reported in the HPTS assay must arise from transmembrane anion transport ($OH^-/Cl^-$ antiport, or $H^+/Cl^-$ symport), and not from $H^+/M^+$ cation antiport, in agreement with the mode of action of previously reported squaramide anion carriers.[17]

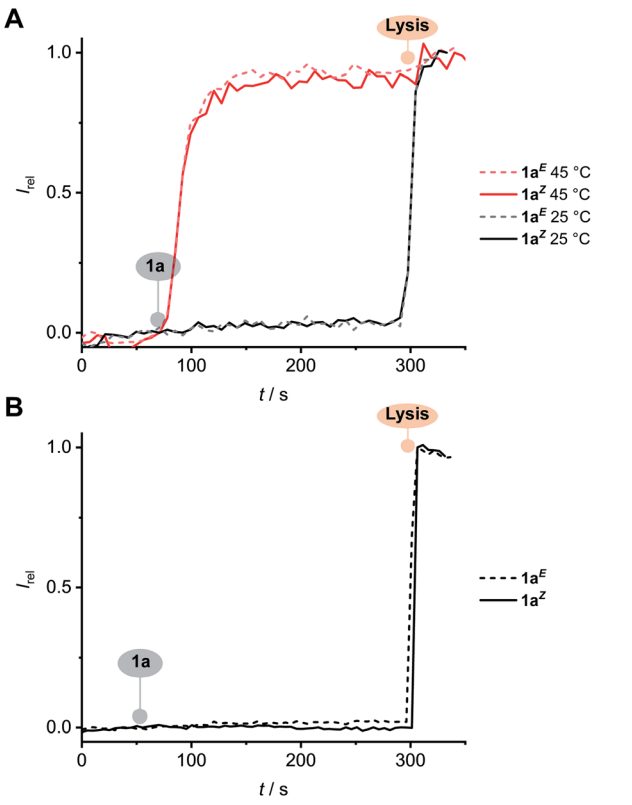


Fig. 6 (A) HPTS assay with DPPC LUVs: 200 nM $\mathbf{1a}^{E}$ (dashed lines) and 62.5 nM $\mathbf{1a}^{Z}$ (solid lines) at 25 °C (black data) and 45 °C (red data). (B) Calcein release assay with 5 μM $\mathbf{1a}^{E}$ (dashed line) and $\mathbf{1a}^{Z}$ (solid line) in POPC LUVs.

Anion transport by $\mathbf{1a}^{E}$ and $\mathbf{1a}^{Z}$ in the lipid gel phase of dipalmitoylphosphatidylcholine (DPPC) lipids at 25 °C was inhibited and restored at 45 °C, above the gel–liquid phase transition temperature ($T_c = 41$ °C) (Fig. 6A). This behaviour is consistent with the proposed mobile carrier mechanism, in which mobility is significantly reduced in the gel phase, and rules out alternative formation of a membrane spanning channel structure whose activity would be independent of the lipid phase. Inactivity in the calcein release assays further rules out carrier-induced non-specific leakage (Fig. 6B).

### Reversible photo-switching of anion transport

To investigate *in situ*, reversible photo-switching of ion transport in vesicles, we measured the transporter-induced chloride efflux from POPC vesicles containing buffered NaCl, suspended in $NaNO_3$ in real time using a chloride ion selective electrode (ISE). Sample illumination was achieved using high powered LEDs (see ESI† for details). Initial studies confirmed that the system could facilitate $Cl^-/NO_3^-$ antiport in this assay, following external addition of the $\mathbf{1a}^{Z}$-rich PSS, with minimal background transport by $\mathbf{1a}^{E}$ in this assay (Fig. S145†).

Reversible control over ion transport by *in situ* photo-switching of **1a** in the vesicle membrane was achieved by adding $\mathbf{1a}^{E}$ as a DMSO solution (0.5 mol% relative to lipid) to the gently stirred vesicle suspension. Irradiation with red light (625 nm) was used to photo-isomerise the transporter within the lipid bilayer membrane, and turn-on the $Cl^-/NO_3^-$ transmembrane transport process, which could be turned off by subsequent irradiation with blue light (455 nm) (Fig. 7). The rate of ion transport following *in situ* photo-isomerisation in the vesicles was ~50% of that achieved by direct addition of $\mathbf{1a}^{Z,PSS}$.[25]

Alternating between 625 and 455 nm light allowed for reversible switching between the transporting "ON" and inactive states "OFF" states, directly coupling photo-isomerisation with ion transport. Inactivity under alternating red and blue

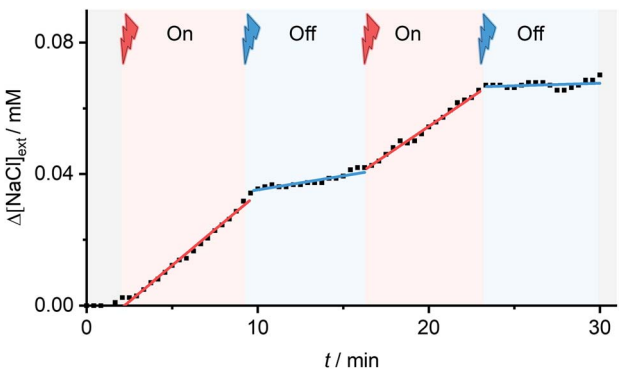


Fig. 7 Photo-triggered ion transport by **1a** (0.5 mol% relative to lipid) from POPC vesicles containing 489 mM NaCl, suspended in 489 mM $NaNO_3$, and buffered with phosphate salts at pH 7.0. Chloride efflux from POPC vesicles monitored by a chloride-selective ISE. Colours indicate commencement of sample irradiation using 625 nM (0.9 W, red) or 455 nm (1.1 W, blue) LEDs. Black squares: vesicle exterior $Cl^-$ concentration; lines: linear fit.

light irradiation in the absence of **1a**; and the lack of switching behaviour when **1a** was replaced with a simple non-photo-responsive squaramide derivative (ESI†), confirmed the role of photo-switch **1a** in the photo-switchable transport behaviour (Fig. S147†).

## Conclusions

We have demonstrated reversible, visible light control over transmembrane anion transport using a synthetic photo-switchable anion carrier. Fluorescence anion transport assays in combination with ISE experiments demonstrate the ability of the squaramide-substituted azobenzenes to act as mobile anion carriers. Switching between the less active *E* isomer and more active *Z* isomer can be achieved with red light, whilst back-switching takes place using blue light; allowing for *in situ*, temporal control over transmembrane ion transport in lipid bilayer vesicles. We anticipate that these results will provide the foundation for developing sophisticated photo-controlled membrane transport systems, with potential longer term impact in targeted therapeutics and synthetic biology.

## Conflicts of interest

There are no conflicts to declare.

## Acknowledgements

A. K. thanks the EPSRC Centre for Doctoral Training in Synthesis for Biology and Medicine for a studentship (EP/L015838/1), generously supported by AstraZeneca, Diamond Light Source, Defence Science and Technology Laboratory, Evotec, GlaxoSmithKline, Janssen, Novartis, Pfizer, Syngenta, Takeda, UCB and Vertex. MJL acknowledges funding from the Royal Society, the John Fell Oxford University Press Research Fund, the University of Oxford's EPSRC Capital Award in Support of Early Career Researchers (EP/S017658/1), and SCG Chemicals Co. Ltd. for funding through the SCG-Oxford Centre of Excellence in Chemistry: SCG Innovation Fund. M. J. L. is a Royal Society University Research Fellow.

## Notes and references

1 G. Miesenböck, *Annu. Rev. Cell Dev. Biol.*, 2011, **27**, 731–758.
2 (*a*) W. A. Velema, W. Szymanski and B. L. Feringa, *J. Am. Chem. Soc.*, 2014, **136**, 2178–2191; (*b*) K. Hüll, J. Morstein and D. Trauner, *Chem. Rev.*, 2018, **118**, 10710–10747.
3 (*a*) G. Villar, A. D. Graham and H. Bayley, *Science*, 2013, **340**, 48–52; (*b*) Y. Elani, R. V. Law and O. Ces, *Ther. Delivery*, 2015, **6**, 541–543; (*c*) K. P. Adamala, D. A. Martin-Alarcon, K. R. Guthrie-Honea and E. S. Boyden, *Nat. Chem.*, 2017, **9**, 431–439.
4 For recent reviews see: (*a*) J. T. Davis, O. Okunola and R. Quesada, *Chem. Soc. Rev.*, 2010, **39**, 3843–3862; (*b*) S. Matile, A. V. Jentzsch, J. Montenegro and A. Fin, *Chem. Soc. Rev.*, 2011, **40**, 2453–2474; (*c*) P. A. Gale, J. T. Davis and R. Quesada, *Chem. Soc. Rev.*, 2017, **46**, 2497–2519.
5 (*a*) B. Díaz de Greñu, P. I. Hernández, M. Espona, D. Quiñonero, M. E. Light, T. Torroba, R. Pérez-Tomás and R. Quesada, *Chem.–Eur. J.*, 2011, **17**, 14074–14083; (*b*) S.-K. Ko, S. K. Kim, A. Share, V. M. Lynch, J. Park, W. Namkung, W. Van Rossom, N. Busschaert, P. A. Gale, J. L. Sessler, *et al.*, *Nat. Chem.*, 2014, **6**, 885–892; (*c*) V. Soto-Cerrato, P. Manuel-Manresa, E. Hernando, S. Calabuig-Fariñas, A. Martínez-Romero, V. Fernández-Dueñas, K. Sahlholm, T. Knöpfel, M. García-Valverde, A. M. Rodilla, *et al.*, *J. Am. Chem. Soc.*, 2015, **137**, 15892–15898; (*d*) H. Li, H. Valkenier, L. W. Judd, P. R. Brotherhood, S. Hussain, J. A. Cooper, O. Jurček, H. A. Sparkes, D. N. Sheppard and A. P. Davis, *Nat. Chem.*, 2016, **8**, 24–32.
6 (*a*) J.-Y. Chen and J.-L. Hou, *Org. Chem. Front.*, 2018, **5**, 1728–1736; (*b*) P. V. Jog and M. S. Gin, *Org. Lett.*, 2008, **10**, 3693–3696; (*c*) T. Liu, C. Bao, H. Wang, Y. Lin, H. Jia and L. Zhu, *Chem. Commun.*, 2013, **49**, 10311–10313; (*d*) Y. Zhou, Y. Chen, P.-P. Zhu, W. Si, J.-L. Hou and Y. Liu, *Chem. Commun.*, 2017, **53**, 3681–3684; (*e*) V. Gorteau, F. Perret, G. Bollot, J. Mareda, A. N. Lazar, A. W. Coleman, D.-H. Tran, N. Sakai and S. Matile, *J. Am. Chem. Soc.*, 2004, **126**, 13592–13593; (*f*) P. Talukdar, G. Bollot, J. Mareda, N. Sakai and S. Matile, *Chem. - Eur. J.*, 2005, **11**, 6525–6532; (*g*) C. P. Wilson and S. J. Webb, *Chem. Commun.*, 2008, **34**, 4007–4009; (*h*) U. Devi, J. R. D. Brown, A. Almond and S. J. Webb, *Langmuir*, 2011, **27**, 1448–1456.
7 (*a*) I. M. Bennett, H. M. V. Farfano, F. Bogani, A. Primak, P. A. Liddell, L. Otero, L. Sereno, J. J. Silber, A. L. Moore, T. A. Moore, *et al.*, *Nature*, 2002, **420**, 398–401; (*b*) N. Busschaert, R. B. P. Elmes, D. D. Czech, X. Wu, I. L. Kirby, E. M. Peck, K. D. Hendzel, S. K. Shaw, B. Chan, B. D. Smith, *et al.*, *Chem. Sci.*, 2014, **5**, 3617; (*c*) Y. R. Choi, B. Lee, J. Park, W. Namkung and K.-S. Jeong, *J. Am. Chem. Soc.*, 2016, **138**, 15319–15322; (*d*) X. Wu, J. R. Small, A. Cataldo, A. M. Withecombe, P. Turner and P. A. Gale, *Angew. Chem., Int. Ed.*, 2019, **58**, 15142–15147 For a visible light responsive cation transporters see: (*e*) T. Jin, *Mater. Lett.*, 2007, **61**, 805–808; (*f*) Y. Rin Choi, G. Chan Kim, H.-G. Jeon, J. Park, W. Namkung and K.-S. Jeong, *Chem. Commun.*, 2014, **50**, 15305–15308; (*g*) S. B. Salunke, J. A. Malla and P. Talukdar, *Angew. Chem., Int. Ed.*, 2019, **58**, 5354–5358.
8 S. Shinkai, T. Nakaji, T. Ogawa, K. Shigematsu and O. Manabe, *J. Am. Chem. Soc.*, 1981, **103**, 111–115.
9 For selected recent reviews on molecular machines including those exploiting photo-switches see: (*a*) S. Erbas-Cakmak, D. A. Leigh, C. T. McTernan and A. L. Nussbaumer, *Chem. Rev.*, 2015, **115**, 10081–10206; (*b*) V. Blanco, D. A. Leigh and V. Marcos, *Chem. Soc. Rev.*, 2015, **44**, 5341–5370; (*c*) L. van Dijk, M. J. Tilby, R. Szpera, O. A. Smith, H. A. P. Bunce and S. P. Fletcher, *Nat. Rev. Chem.*, 2018, **2**, 1–18.
10 A. A. Beharry and G. A. Woolley, *Chem. Soc. Rev.*, 2011, **40**, 4422–4437.
11 (*a*) V. Saggiomo, S. Otto, I. Marques, V. Félix, T. Torroba and R. Quesada, *Chem. Commun.*, 2012, **48**, 5274–5276; (*b*) N. Busschaert, S. J. Bradberry, M. Wenzel, C. J. E. Haynes,

 

J. R. Hiscock, I. L. Kirby, L. E. Karagiannidis, S. J. Moore, N. J. Wells, J. Herniman, *et al.*, *Chem. Sci.*, 2013, **4**, 3036–3045.

12 X. Wu, L. W. Judd, E. N. W. Howe, A. M. Withecombe, V. Soto-Cerrato, H. Li, N. Busschaert, H. Valkenier, R. Pérez-Tomás, D. N. Sheppard, *et al.*, *Chem*, 2016, **1**, 127–146.

13 S. J. Edwards, I. Marques, C. M. Dias, R. A. Tromans, N. R. Lees, V. Félix, H. Valkenier and A. P. Davis, *Chem. - Eur. J.*, 2016, **22**, 2004–2011.

14 H. M. Dhammika Bandara and S. C. Burdette, *Chem. Soc. Rev.*, 2012, **41**, 1809–1825.

15 (*a*) A. A. Beharry, O. Sadovski and G. A. Woolley, *J. Am. Chem. Soc.*, 2011, **133**, 19684–19687; (*b*) M. J. Hansen, M. M. Lerch, W. Szymanski and B. L. Feringa, *Angew. Chem., Int. Ed.*, 2016, **55**, 13514–13518; (*c*) D. Bléger, J. Schwarz, A. M. Brouwer and S. Hecht, *J. Am. Chem. Soc.*, 2012, **134**, 20597–20600; (*d*) S. Samanta, A. A. Beharry, O. Sadovski, T. M. McCormick, A. Babalhavaeji, V. Tropepe and G. A. Woolley, *J. Am. Chem. Soc.*, 2013, **135**, 9777–9784; (*e*) M. Dong, A. Babalhavaeji, M. J. Hansen, L. Kálmán and G. A. Woolley, *Chem. Commun.*, 2015, **51**, 12981–12984.

16 K. Dąbrowa, P. Niedbała and J. Jurczak, *Chem. Commun.*, 2014, **50**, 15748–15751.

17 N. Busschaert, I. L. Kirby, S. Young, S. J. Coles, P. N. Horton, M. E. Light and P. A. Gale, *Angew. Chem., Int. Ed.*, 2012, **51**, 4426–4430.

18 A. Antoine John and Q. Lin, *J. Org. Chem.*, 2017, **82**, 9873–9876.

19 P. Kuzmič, *Anal. Biochem.*, 1996, **237**, 260–273.

20 C. Hansch, A. Leo and R. W. Taft, *Chem. Rev.*, 1991, **91**, 165–195.

21 Note that the measured $EC_{50}^{Z,PSS}$ is an underestimate of the intrinsic transport ability of $\mathbf{1}^{Z}$, with the actual activity ~1.25× higher ($EC_{50}$ 0.8× smaller) due to the incomplete isomerisation to the Z isomer in the PSS.

22 E. L. Doyle, C. A. Hunter, H. C. Phillips, S. J. Webb and N. H. Williams, *J. Am. Chem. Soc.*, 2003, **125**, 4593–4599.

23 Compatibility of the dose–response curves with the Hill equation with Hill coefficients $n > 1$ reveals endergonic self-assembly (un-stable supramolecules) and provides information on the stoichiometry; $n = 1$ or $n < 1$ reveals exergonic self-assembly (stable supramolecules). See S. Bhosale and S. Matile, *Chirality*, 2006, **18**, 849–856.

24 N. Sakai and S. Matile, *J. Phys. Org. Chem.*, 2006, **19**, 452–460.

25 Similar results were obtained for *in situ* photo-isomerisation of $\mathbf{1a}^{E}$ in the HPTS assay. See ESI† for further details.